



LAWRENCE
LIVERMORE
NATIONAL
LABORATORY

FLASH X-RAY (FXR) LINEAR INDUCTION ACCELERATOR (LIA) OPTIMIZATION

Upgrade of the OTR Emittance Diagnostic

T. L. Houck, P. E. Wargo

December 21, 2006

Disclaimer

This document was prepared as an account of work sponsored by an agency of the United States Government. Neither the United States Government nor the University of California nor any of their employees, makes any warranty, express or implied, or assumes any legal liability or responsibility for the accuracy, completeness, or usefulness of any information, apparatus, product, or process disclosed, or represents that its use would not infringe privately owned rights. Reference herein to any specific commercial product, process, or service by trade name, trademark, manufacturer, or otherwise, does not necessarily constitute or imply its endorsement, recommendation, or favoring by the United States Government or the University of California. The views and opinions of authors expressed herein do not necessarily state or reflect those of the United States Government or the University of California, and shall not be used for advertising or product endorsement purposes.

This work was performed under the auspices of the U.S. Department of Energy by University of California, Lawrence Livermore National Laboratory under Contract W-7405-Eng-48.

**FLASH X-RAY (FXR)
LINEAR INDUCTION ACCELERATOR (LIA)
OPTIMIZATION**

Upgrade of the OTR Emittance Diagnostic

Tim Houck (LLNL)

Paul Wargo (Bechtel Nevada)

December 2006

Table of Contents

Abstract	3
Introduction	3
Optical Package	4
Foil, Cameras, and Fiber Bundle	5
Calibration	6
Summary	8
Acknowledgements	10
References	10
A. Custom Lens	11
B. Spot Diagram	12
C. Lens Holder Assembly	13
D. Specifications & Drawings for Fiber Optic Bundle	14

Abstract

Knowing the electron beam parameters at the exit of an accelerator is critical for several reasons. Foremost is to optimize the application of the beam, which is flash radiography in the case of the FXR accelerator. The beam parameters not only determine the theoretical dose, x-ray spectrum, and radiograph resolution (spot size), they are required to calculate the final transport magnetic fields that focus the beam on the bremsstrahlung converter to achieve the theoretical limits. Equally important is the comparison of beam parameters to the design specifications. This comparison indicates the “health” of the accelerator, warning the operator when systems are deteriorating or failing.

For an accelerator of the size and complexity of FXR, a large suite of diagnostics is normally employed to measure and/or infer beam parameters. These diagnostics are distributed throughout the accelerator and can require a large number of “shots” (measurements) to calculate a specific beam parameter. The OTR Emittance Diagnostic, however, has the potential to measure all but one of the beam parameters simultaneously at a specific location. Using measurements from a scan of a few shots, this final parameter can also be determined. Since first deployment, the OTR Emittance Diagnostic has been limited to measuring only one of the seven desired parameters, the beam’s divergence. This report describes recent upgrades to the diagnostic that permit full realization of its potential.

Introduction

The objective of the FXR Optimization Project is to generate an x-ray pulse with peak energy of 19 MeV, spot-size of 1.5 mm, dose of 500 rad, and duration of 60 ns. To achieve this small spot-size while maintaining the dose, i.e. without the use of an x-ray collimator, the emittance of the electron beam must be minimized and the final beam transport optimized. Diagnostics that can determine the various beam parameters at the exit of the accelerator are obviously needed both to achieve the smallest x-ray spot possible with the existing beam and to determine if the beam quality is changing.

The principle diagnostics for measuring beam parameters have been voltage monitors, resistive wall current monitors (beam bugs), and an intercepting foil inserted into the drift section of FXR. Imaging the light created as the beam passes through the foil allows the current density to be determined from which the radius of the beam is then calculated. Observing the change in radius as upstream transport magnets are varied, and knowing the beam energy and current, allows the beam parameters to be estimated including the emittance. A more direct measurement of the emittance is possible by imaging the Optical Transition Radiation (OTR) angular intensity distribution from the intercepting foil. A diagnostic, referred to as the OTR Emittance Diagnostic, for performing this measurement has been developed and deployed at FXR^{i,ii}. The diagnostic has been successful at determining an upper limit on the emittance, but has not been utilized to its full potential.

Low signal to noise ratios, inability to simultaneously acquire current density and OTR angular distributions, and unknown “waist” conditions have limited the full capability of the diagnostic. This report describes recent upgrades to the existing

emittance diagnostic system. Sufficient detail is provided to allow repairs, replacement, and/or upgrades to be made. The improvements allow the diagnostic to be used real time for measuring all beam parameters including the emittance as adjustments are being performed to the acceleratorⁱⁱⁱ.

Optical Package

The previous optics design placed a thin, frosted quartz disc at the focal plane of a pair of achromat lenses such that parallel light rays were focused to a point on the disc. A commercial Nikon 35 mm lens was then used to focus the disc image onto a fiber optic bundle that coupled the image onto the camera. The primary issue with this design was lost of light leading to low intensity and signal to noise ratio at the camera. It was realized that significant improvement in the image intensity at the camera could be gained if the OTR angular distribution was imaged directly onto the fiber bundle. In addition, the previous design was housed in a meter long lens holder fabricated from Delrin®. There was a desire to package the lens system in a more compact and rigid housing to improve alignment. To ease the constraints on the new optical design, the full angular field of view was reduced from ± 12 degrees to ± 6 degrees. The smaller field of view does not impact the accuracy and has the advantage of improving the angular resolution of the OTR light distribution.

The new optics design is shown in Figure 1. The general design specifications for the new optical system were:

Wavelength: 450nm–600nm (visible light range)

Full field of view: ± 6 degrees ($\pm 4/\gamma$)

Fiber bundle size: 14mm x 14mm (active area at focal plane)

Resolution across field: 70 micron diameter

Maximum beam spot on foil: 20mm diameter (beam edge radius = 1 cm)

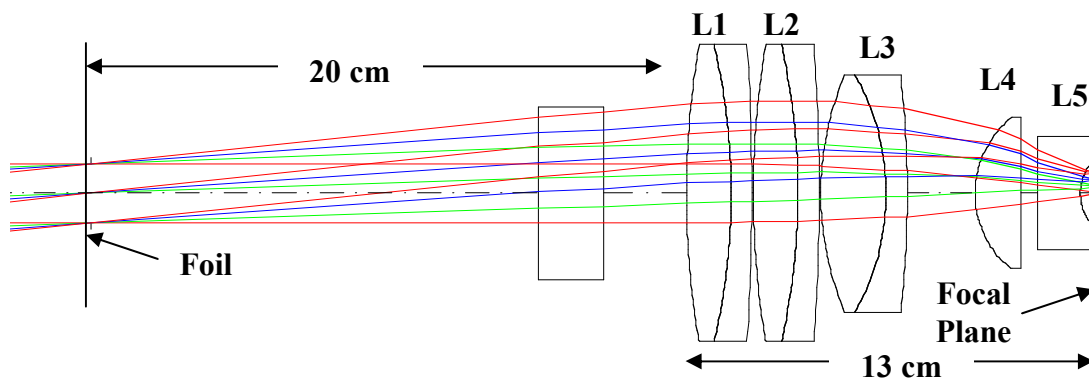


Figure 1. Optics system showing ray traces for 0 to 6 degrees originating at foil.

The lenses used in the new design are:

L1: Linos #322316 achromat (EFL = 500mm, diameter = 100mm) from original design

L2: Linos #322316 achromat (EFL = 500mm, diameter = 100mm) from original design

L3: Linos #322267 achromat (EFL = 160mm, diameter = 80mm)

L4: Newport #KPX178AR.14 singlet (EFL = 500mm, diameter = 100mm)

L5: Custom SF11 (EFL = -12.8mm, diameter = 14.7mm) refer to Appendix A

A “spot” diagram showing the calculated focus of different light wavelengths for various angles/offsets is provided in Appendix B. Some improvement in spot size could be made with the use of filters, but all wavelengths were within the design specification of 70 microns. A photograph of the assembled lens array positioned on the alignment table is shown in Figure 2. A mechanical assembly drawing of the lens holder is given in Appendix C.

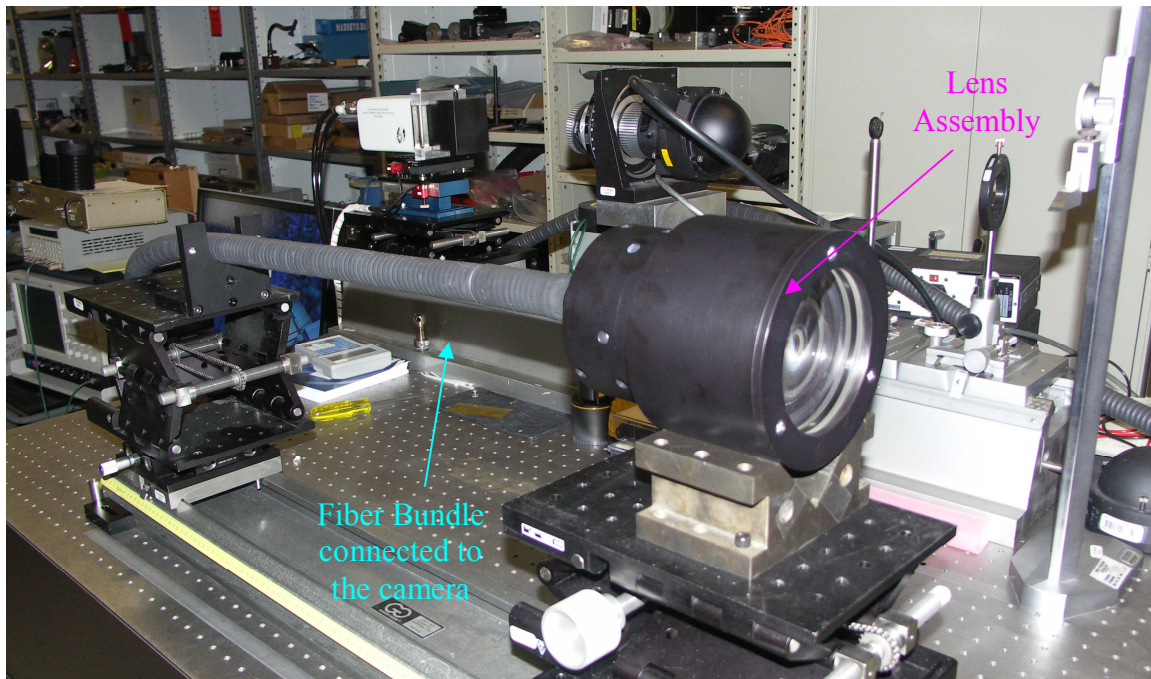


Figure 2. Photograph of the OTR Optics package on the calibration bench.

Foil, Cameras, and Fiber Bundle

The OTR angular distribution is used with the current distribution, specifically the beam radius, to determine the emittance. In addition to the change in the OTR optical package, the beam intercepting foil was modified to allow imaging from both front and back surfaces. The foil is a 15 mil thick, 4.375 inch diameter, quartz disc polished on one side^{iv}. Reference 2 provides an analysis of damage threshold as a function of minimum beam diameter for several foil materials. A 1,200 Å aluminum layer is vapor deposited on the polished side. This surface is used for imaging the OTR angular distribution. On the opposite (nonpolished or ground) side of the foil, a fast scintillator phosphor (ZnO:Ga, 2 ns decay time) layer was applied with a sprayer to a depth of about 10 mils. This side of the foil was imaged with a commercial Nikon 60 mm lens that focuses the beam image onto a fiber optic bundle. The nonpolished foil surface has a ground finish of 64 micro inches and the thinness of the quartz makes it difficult to increase the surface roughness. Attempts to image the scattered Cherenkov light from the foil surface with no phosphor produced a low intensity signal. OTR light exiting the foil is in the direction of the beam and is not scattered. The phosphor has proven to be mechanically as robust as the

aluminum on the front surface and yields a much more intense light in the direction of the optics.

Fiber bundles were used to transfer the light from the back of the optical packages to the respective cameras. The bundles are comprised of 60-micron square multifibers using 6X6 arrays of 36 10-micron fibers (pixels). The active area is 14 mm by 14 mm with a numerical aperture (NA) of 0.63. Full specifications for the fiber bundle as well as assembly drawings are given in Appendix D.

The images are recorded with Princeton Instruments PI-MAX gated, intensified CCD cameras. For calibration purposes the camera is gated between a few 100 microseconds to a few milliseconds. During operations when imaging beam signals, the camera is gated at 2 ns. The cameras systems are located in electromagnetically shielded cases including approximately 4 inches of lead when used in the FXR accelerator hall. Gamma radiation produced from beam electrons striking the interior of the accelerator beam line produce noise spikes (starring or speckles) in the individual CCD elements. Additional, localized lead shielding reduces this noise.

Calibrations

Two different calibrations were performed. First was the measurement of pixel location with respect to ray angle. Figure 3 shows a schematic of the equipment layout for performing this calibration. A HeNe laser beam was reflected off a mirror into the OTR Optics Package to represent light from the center of the foil. By adjusting the angle of the mirror, we could simulate the beam induced OTR light leaving the foil at different angles. Results of this calibration are shown in Figure 4. Measurements were recorded for 0.25° increments from -3° to $+3^\circ$ about the nominal 45° (0° with respect to the package optical axis) position. Note that a 0.25° rotation represents a 0.5° change with respect to entry into the optics. Figure 4a is an overlay of the 25 calibration images, cropped to display a 1023×60 pixel strip across the image, and with the maximum intensity level limited to about 5,000 counts above background so that all the images have the same peak intensity. Figures 4b and 4c show a close up of a single calibration image (21 by 21 pixels). Figure 4d is a lineout of 4a prior to limiting the intensity level to show relative intensities. There is some variation in spacing between the peaks, assumed due to the difficulty in rotating the mirror in 0.25° increments, but on average the calibration is 0.0121° per pixel. This calibration corresponds to a “flat” field for the angular distribution at the focal plane similar to the more usual “flat” field performed at the image plane. For an ideal system, the intensities shown in Figure 4d would be equal. A more complete calibration would involve repeating the measurements with the mirror translated with respect to the Optics package such that the nominal 45° degree case had the laser beam entering the optics parallel, but offset to the axis.

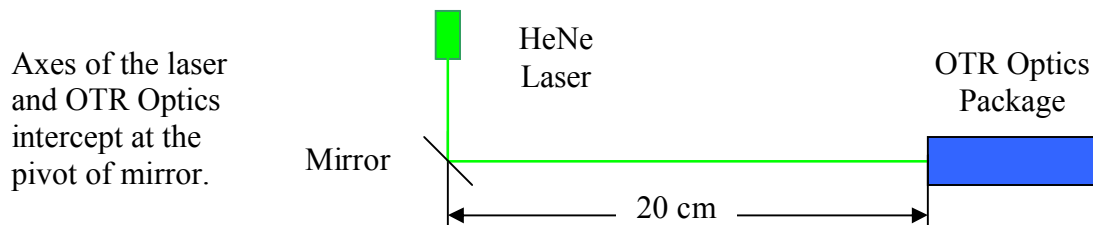


Figure 3. Schematic of equipment setup for the calibration of the OTR Optics.

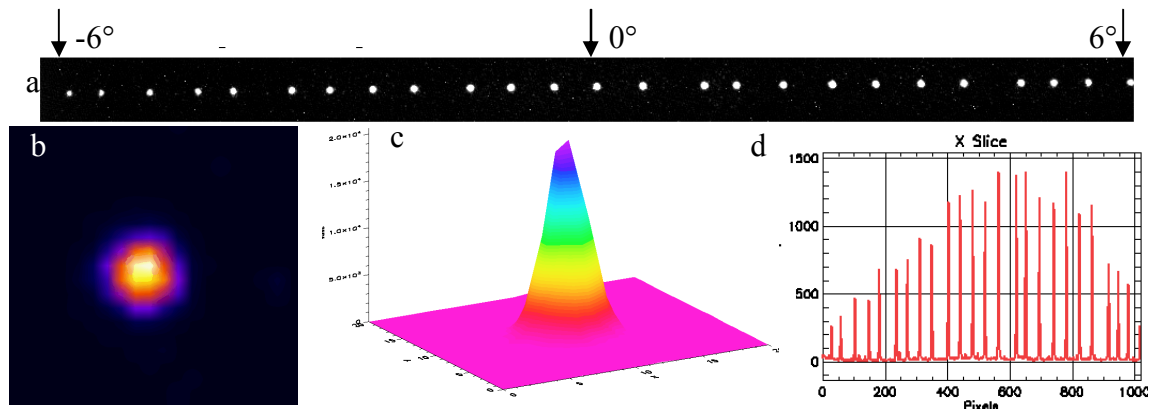
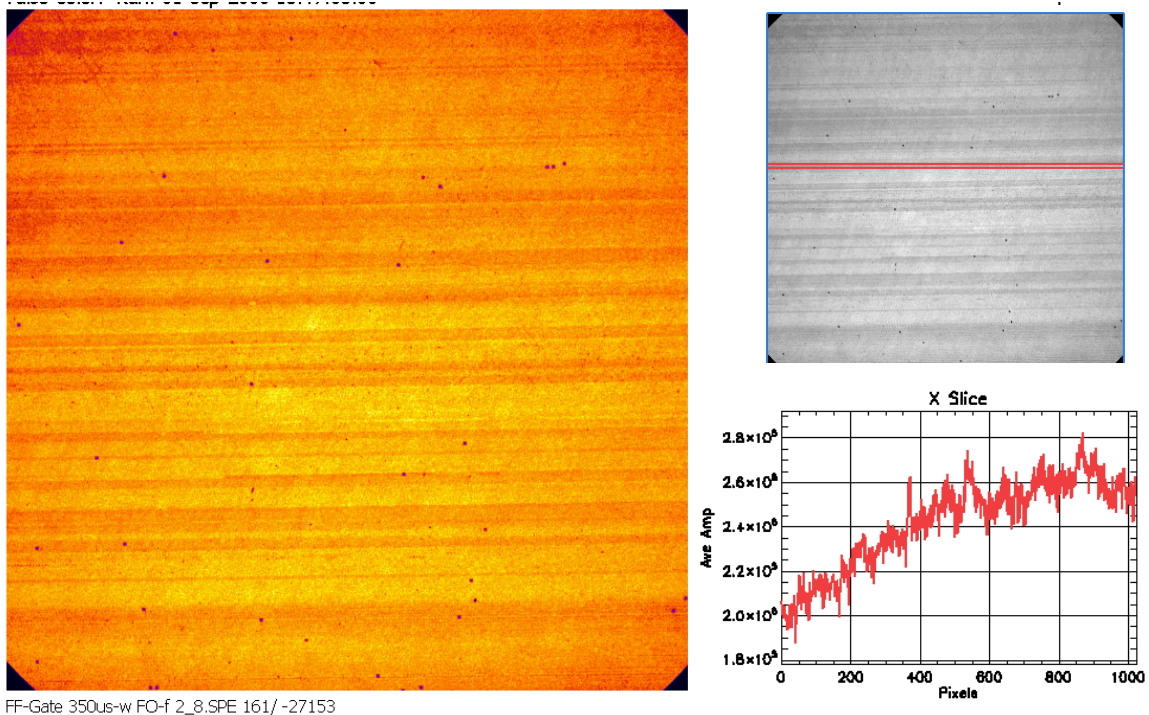


Figure 4. Sample calibration measurements: a) cropped (1023x60 pixels) composite image of 25 calibration images, b) close up (21x21 pixels) of single calibration image, c) surface plot of b, d) relative peak intensity of calibration images.

The second calibration measured the flatness of the camera and fiber optic bundle. The end of the fiber optic bundle was mounted to an integrating sphere. A typical flat field image is shown in Figure 5. A lineout, taken across the image at the same vertical position as the angular calibration images, is also shown. Note that the vertical axis zero is suppressed so the variation from minimum to maximum normalized to the average value is approximately 20%.



FF-Gate 350us-w FO-f 2_8.SPE 161/ -27153

Figure 5. Flat field of fiber optic bundle/camera system. Note the depressed zero on the vertical scale of the lineout.

Measurements

A “before and after comparison” of data is the most direct method for appreciating the improvement to the OTR diagnostic. An OTR image taken on 3/31/2006 with the previous OTR Optics package is shown on the left in Figure 6 while an image taken 6/2/2006 with the new optics is shown on the right. Both images were taken with nominal accelerator operating parameters and should be identical except for the new optics. Most noticeable between the two images is the increase in peak intensities. With the new optics it is necessary to reduce the intensity of the OTR light reaching the CCD to avoid saturation. Less obvious, but more important, the average background, measured by rotating the intercepting foil so that the OTR light is outside the acceptance of the optics, dropped from 1,500 counts with the old system to 1,000 counts. The figure of merit for beam quality based on emittance is the ratio of the central minimum to peak intensity. Thus the most important signal to noise ratio is that of the central minimum to the background. With the new optics, this ratio was improved by almost a factor of 3 and the estimate of the maximum emittance can be reduced by about 30%.

For completeness Figure 7 displays the image of the phosphor coated, backside of the foil taken on the same shot as the OTR distribution image of 6/2/2006 shown in Figure 6. Obviously no corresponding image is available for the previous package. The rms beam radius in this image is 1 cm. The peak intensity of the image is approximately one half of the full scale using an fstop of 11 and full intensifier gain. The gain and fstop had been adjusted so that the beam could be focused to a radius of 7 mm prior to saturating the camera. At radii smaller than 7 mm there is a danger of damaging the Aluminum coating on the foil and at a radius less than 5 mm the foil is damaged.

Summary

The improved signal intensity and reduced signal to noise ratio allow more accurate measurements of the OTR angular distribution. The second camera system and changes to the foil allow the simultaneous measurement of the beam’s current distribution. The two images together provide a wealth of information about the beam:

1. The peak-to-peak angular spread in the OTR distribution as seen in Figure 6 is equal to $2/\gamma$ and thus is a measurement of the beam energy.
2. The ratio of the central minimum intensity to the peak intensity in the OTR angular distribution provides a measurement of the beam’s divergence.
3. The physical position of the central minimum with respect to the center of the image is a measurement of the angle between the beam’s trajectory and the accelerator’s mechanical axis.
4. The intensity of the scintillation imaged on the back of the foil is proportion to the electrons striking the phosphor and is a measurement of the beam current density distribution. The beam moments can be calculated directly from this distribution, e.g. radius.
5. The integration of the scintillation intensity is proportional to the beam current and can be calibrated to measure absolute current.

- The physical position of the light distribution with respect to the center of the image is a measurement of the beam's position with respect to the accelerator's mechanical axis.

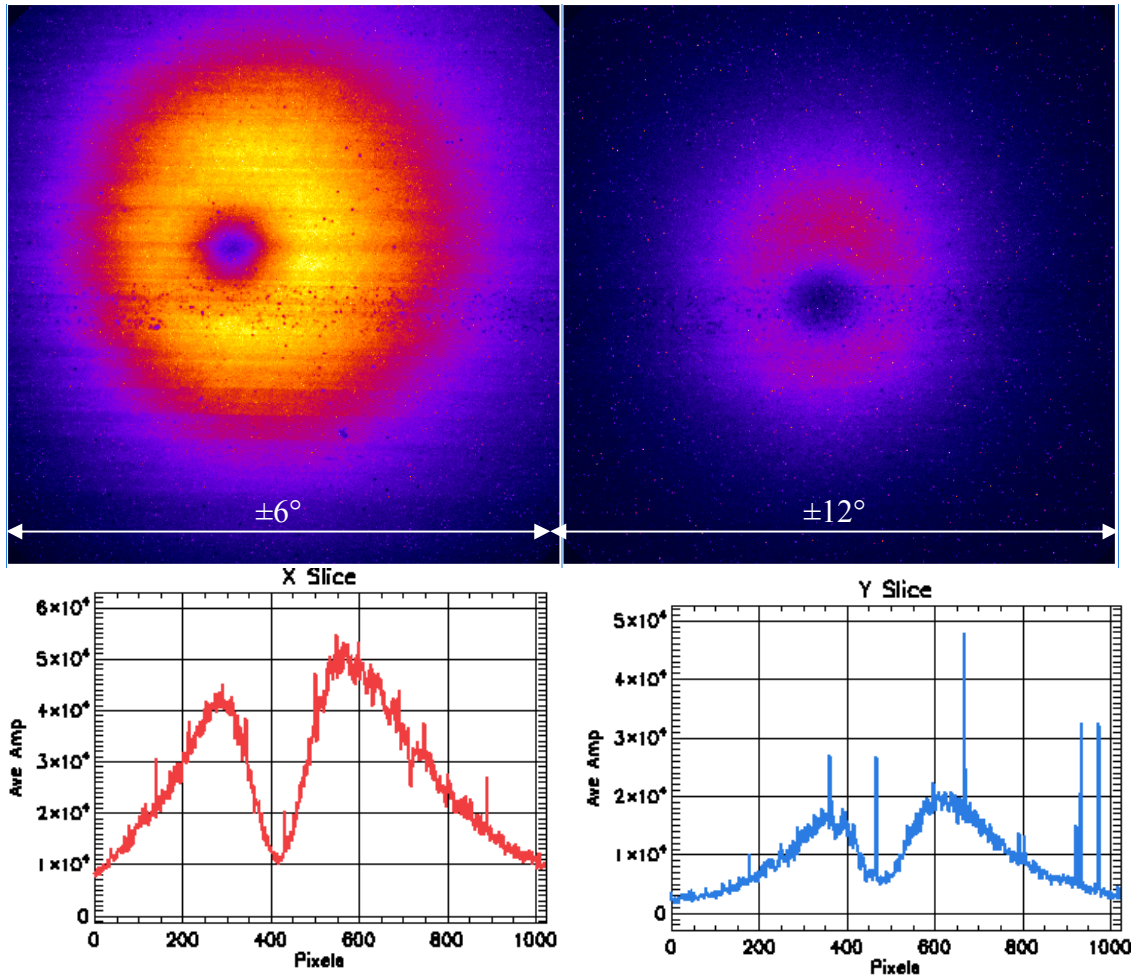
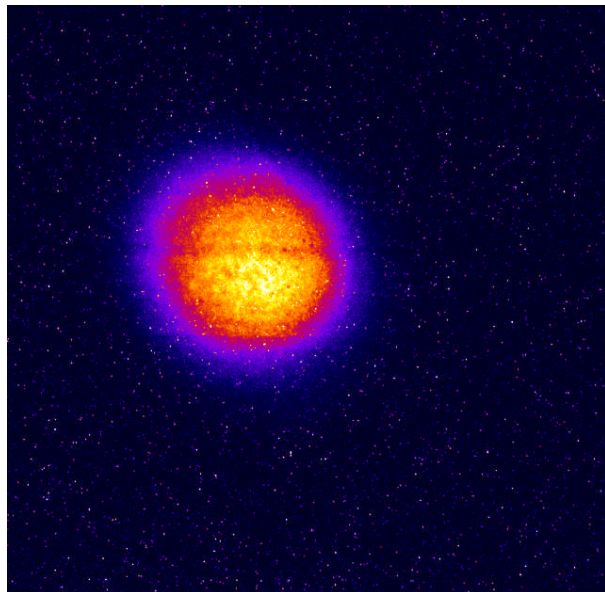


Figure 6. OTR angular intensity distributions for the upgraded system (left) and original system with lineouts passing through the central minimum and maximum intensities.

Figure 7. Shown to the left is the image of the back of the foil taken with the OTR image shown in Figure 6 (left). The light is due to the scintillation of the phosphor by the beam. The rms radius of the beam is approximately 1 cm.



The final parameter needed to fully characterize the beam is the tilt of the phase space ellipse. The tilt is related to whether the beam envelop is decreasing to a smaller diameter, expanding to a larger diameter, or is at a minimum/maximum as it passes through the intercept foil. Several measurements with different upstream transport parameters allow the tilt to be inferred. Reference 3 provides definitions of the beam parameters and details of the methodology for determining these parameters from the OTR Emittance Diagnostic.

It should be stressed that this diagnostic determines all the beam parameters at one location eliminating the uncertainties/errors when measurements from diagnostics at various locations are used. However, the OTR Emittance Diagnostic is not a replacement for the more sensitive energy spectrometer and resistive wall current monitor. The energy and current should not change between the exit of the accelerator and the bremsstrahlung converter so the location of measurement is not critical.

Acknowledgements

Many people assisted in the diagnostic upgrade. Unless otherwise noted, the following individuals are LLNL employees. Nan Wong and Lynn Seppala designed the optics. Lynn Seppala also did the design for the original diagnostic. Roger Van Maren and Chuck Cadwalader applied the Al coating to the quartz disc. Cliff Holmes applied the phosphor to the back of the quartz disc. Al Traille (Bechtel Nevada, Livermore Office), Charles Brown, and Obi Ohia (summer intern from Iowa State University) assisted with the calibration of the optics package. Al Traille also helped with the equipment setup at the FXR facility.

Testing of the upgraded diagnostic was done at the FXR facility. Keith Lewis installed the foil and did final modifications to the mounting flanges that attached the lens holder to the diagnostic port. Jan Zentler (FXR Engineer) and Blake Kreitzer (Operator) operated the accelerator and provided beam on request. Ed Koh provided assistance with the camera data acquisition computers. Sean Watson operated the cameras and acquired the images shown in Figure 6 and 7.

References

ⁱ G.P. LeSage, et al., "Time-resolved emittance characterization of an induction linac using Optical Transition Radiation," LLNL, UCRL-ID-153254, 5 November 2002.

ⁱⁱ J.S. Jacob, et al., "Time-resolved OTR Emittance Measurement," LLNL, UCRL-TR-214037, (2005)

ⁱⁱⁱ T.L. Houck, et al., "Tuning the Magnetic Transport of an Induction Linac using Emittance," LLNL, UCRL-CONF-223696, (2006)

^{iv} The disc was manufactured by GM Associates, 9824 Kitty Lane, Oakland, CA 94603, 510-430-0806. The part number is 111-015P1.

Appendix A Specifications & Drawing for the Custom Lens

The lens was fabricated by Applied Optics, Inc. in Pleasant Hill, CA. Our contact person at Applied Optics was Gery Koch, the manager (GeryKoch@applied-optics.com, ph: 925-932-5686 x20, fax: 925-932-2502). Additional information on the company can be found at www.applied-optics.com.

	RADIUS	RAD TOL	POW/IRR	C.A. DIA	EDGE DIA	DIA TOL	CENTRAL THICKNESS	THI TOL	WEDGE
S1	INF	TPF	/	28.233	38.100		10.000		
S2	16.697 CC	TPF	/	18.391					

NOTES :

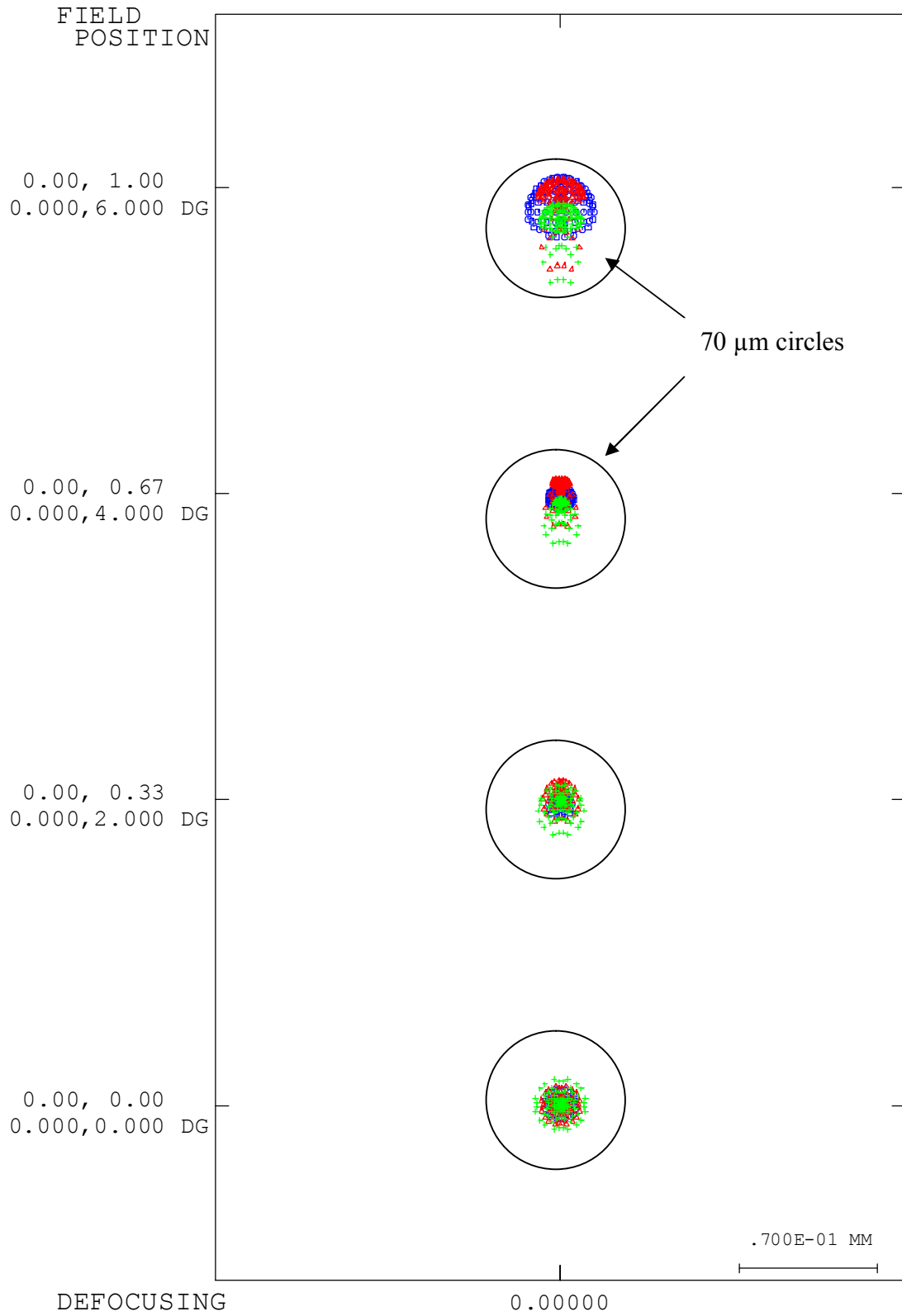
1. ALL DIMENSIONS ARE IN MILLIMETERS.
2. MATERIAL: OPTICAL GLASS PER MIL-G-174
 TYPE: F2 SCHOTT NO. 620364
 n_d 1.6200 ± v 36.4 ±
 STRIAE GRADE , ANNEAL
 MELT NO.
3. 'P' PITCH POLISH TO TEST PLATE WITHIN
 POWER AND IRREGULARITY INDICATED.
4. MANUFACTURE PER MIL-O-13830
5. SURFACE QUALITY
6. 'C' MAGNESIUM FLUORIDE COATING PER MIL-C-675
 FOR MAX TRANSMISSION AT MILLIMICRONS.
7. 'G' FINE GROUND & BLACKENED PER
8. BEVEL EDGES AT 45 DEG TO MAX FACE WIDTH
9. DIAMETER TO FLAT IS (REF)
 WITH SURFACE SAG OF ON SURFACE S2

S1 →

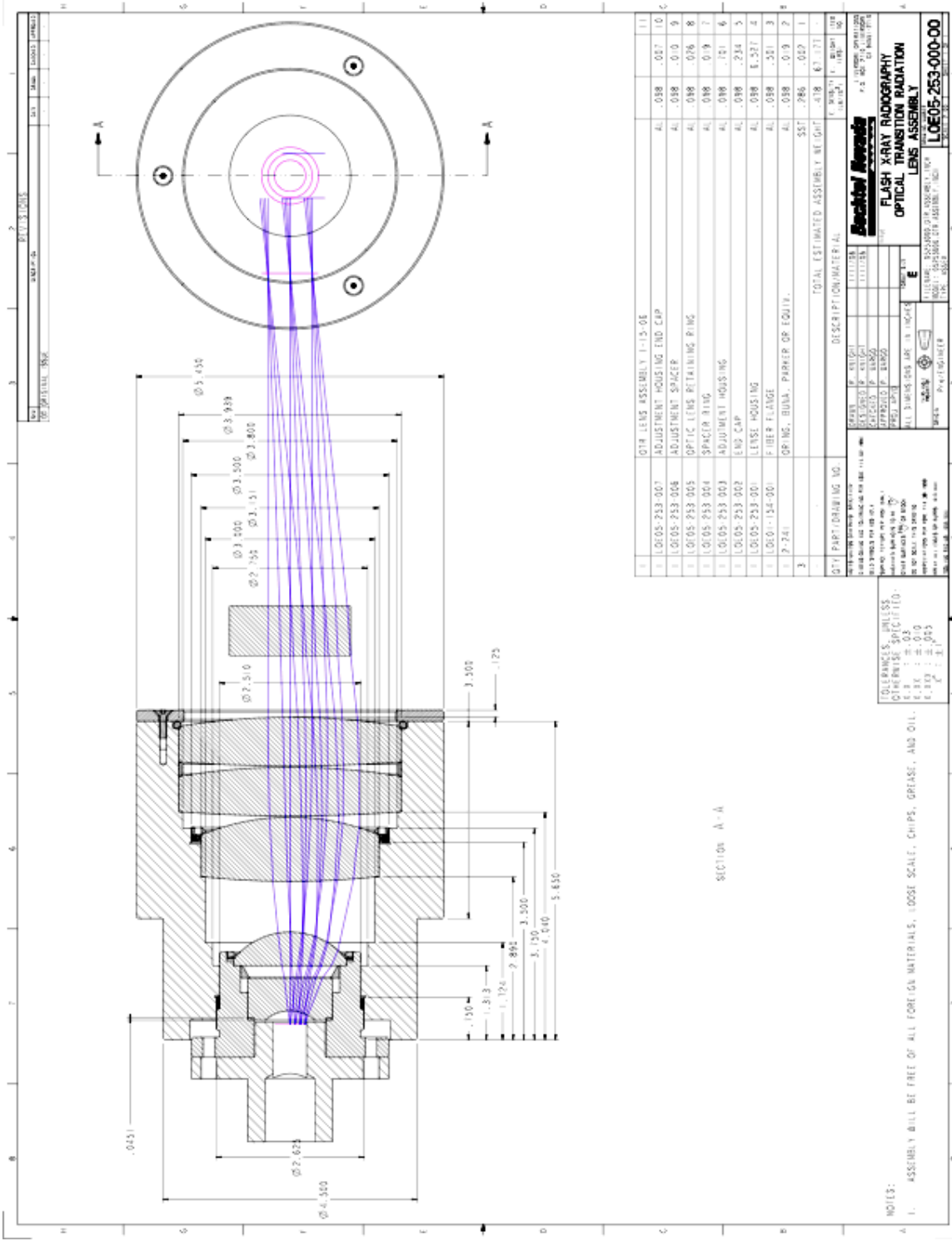
← S2

	DR		
	CHK		
	APPD		
	SCALE	REL BY	REL DATE
ELEMENT 1	2.80:1		-

Appendix B Spot Diagram



Appendix C Lens Holder Assembly Top assembly drawing for the lens holder.



Appendix D
Specifications & Drawings for Fiber Optic Bundle

SCHOTT

Telefax: 925 960 2555

TO: Bechtell Nevada
Mr. Paul Wargo

Lawrence Livermore Natl. Lab
Mr. Mike Ong

CC: Schott Fiber Optics
Mr. Gerald Senecal

Pages: 1

Schott Fiber Optics, Inc.

122 Charlton Street
Southbridge, MA 01550-1960

From: Colleen Bayrouy

Date: February 22, 2001

Phone: (508)765-3316

Fax: (508)764-6273

E-Mail: Bayrouy@sfoinc.com

Web Site: <http://www.schottfiberoptics.com>

RE: Specification for reference number 01-303

Format Size:	15mm x 15mm
Quality Area Size:	14mm x 14mm
Length:	12.5 feet
Numerical Aperture:	.63
Fiber Size:	60-Micron square multifiber, using a 6x6 Array of 36 (10-micron pixels)
Broken fibers:	.2% (121 max) No three adjacent broken fibers No more than one occurrence of two adjacent Broken fibers per 12 square mm of format
Overlays:	No transposed fibers
Coherency:	.001 inch (25 microns)
Endtips:	Aluminum – ref. Drwg # LOE01-145-01
Sheathing:	Stainless steel strip wound, with fiberglass braid and a Silicone rubber outer jacket
End finish:	8 – 12 fringes
Light transmission:	Collimated light, 30% minimum at 420 nanometers (Per SFO "best effort basis")
Uniformity of transmission:	SFO does not have a way to measure this

The endtip diameter of 1.50 inches on the backside
of the endtip may change due to the availability of
sheathing size.

Kind regards,

Colleen Bayrouy
Customer Service
Flexible Department

